PHYSICAL REVIEW A **94**, 043604 (2016)

Quantum correlations in pumped and damped Bose-Hubbard dimers

M. K. Olsen and C. V. Chianca
School of Mathematics and Physics, University of Queensland, Brisbane, Queensland 4072, Australia

K. Dechoum
Instituto da Física, Universidade Federal Fluminense, Boa Viagem 24210-340, Niterói, Rio de Janeiro, Brazil
(Received 7 July 2016; published 3 October 2016)

We propose and analyze two-well Bose-Hubbard models with pumping and losses, finding that these models, with damping and loss able to be added independently to each well, offer a flexibility not found in optical coupled cavity systems. With one well pumped, we find that both the mean-field dynamics and the quantum statistics show a quantitative dependence on the choice of damped well. Both the systems we analyze remain far from equilibrium, preserving good coherence between the wells in the steady state. We find a degree of quadrature squeezing and mode entanglement in these systems. Due to recent experimental advances, it should be possible to demonstrate the effects we investigate and predict.

DOI: 10.1103/PhysRevA.94.043604

I. INTRODUCTION

Recent advances in the techniques of configuring optical potentials [1,2] allow for the fabrication of lattice potentials for ultracold atoms in a variety of geometric configurations. Combined with the technique of causing dissipation from a particular lattice site through use of an electron beam [3] or by optical means [4], and the possibility of pumping a Bose-Hubbard system from a larger reservoir condensate [5,6], we have the elements required for the fabrication of nonlinear damped and pumped atom-optical cavities with varying configurations. In this work we perform theoretical investigations of two different Bose-Hubbard models [7–9] with added pumping and loss. We investigate the population dynamics, the quantum statistics of the system such as squeezing and inseparability, and a pseudoentropy obtained from a reduced single-particle density matrix. We will show that there is some degree of steady-state quadrature squeezing in both the configurations we examine, that mode inseparability is demonstrated using quadrature measures, and that the population dynamics and quantum statistical features depend on both the configuration and the collisional nonlinearity.

An early investigation by Drummond and Walls analyzed a quantum optical system consisting of a Kerr medium inside a Fabry-Pérot cavity, which is mathematically the equivalent of a pumped and damped single isolated well of a Bose-Hubbard model [10], with the main difference being that Kerr nonlinearities tend to be higher with atomic systems. More recently, Pižorn has analyzed Bose-Hubbard models with pumping and dissipation [11], using density-matrix techniques, which are useful for moderate numbers of atoms and wells. Le Boité *et al.* have analyzed a two-dimensional Bose-Hubbard model in terms of steady-state phases and instabilities, with an emphasis on coupled photonic microcavities [12]. More recently, Cui *et al.* have investigated driven and dissipative Bose-Hubbard models, obtaining mean-field analytical results for a two-well system [13]. In this work we analyze both the dynamics and steady-state properties of our systems, going beyond the mean-field approximation with the truncated Wigner representation [14,15], which does not impose a computational limitation on the number of atoms. The main advantages of the truncated Wigner representation are that the computational complexity scales linearly with the number of wells and it does not suffer from the catastrophic instabilities of the positive-P representation [16]. In the present situation, since we are dealing with an open system, the internal states will be mixed and the Wigner function will be strictly positive [17], so we fully expect the truncated Wigner representation to be accurate.

Apart from the fact that we are dealing with condensed atoms, which typically exhibit far higher $\chi^{(3)}$ nonlinearities than those found in optical systems, the major difference between our systems and coupled nonlinear optical cavities [18] is that there is a basic asymmetry built into our systems. Whereas a pumped optical cavity cannot be lossless, a pumped well of a Bose-Hubbard system does not necessarily experience loss. This allows us to assign pumping and loss independently to the wells, using the techniques outlined above. This is a degree of freedom not available with optical systems. We also note here that, while we use the term steady state, this will only hold while the pumping condensate is relatively undepleted.

II. PHYSICAL MODEL, HAMILTONIAN, AND EQUATIONS OF MOTION

In this investigation we use the truncated Wigner representation [14,15], which we fully expect to be accurate for our systems in the presence of pumping and dissipation. Although this method will not capture any revivals in population oscillations in an isolated Bose-Hubbard dimer [19] nor will it calculate two-time correlation functions accurately [20], we do not expect the first in a damped system and we are not interested in the second here. The truncated Wigner representation goes beyond the pairing mean-field theory [21] and the Bogoliubov backreaction method [22–24] previously used in theoretical analyses in that it imposes no factorization assumptions on correlations, irrespective of their order.

Beginning with the two-well unitary Bose-Hubbard Hamiltonian, this is written as

$$\mathcal{H} = \hbar\chi \sum_{i=1}^{2} \hat{a}_i^{\dagger 2}\hat{a}_i^2 - \hbar J(\hat{a}_1^\dagger \hat{a}_2 + \hat{a}_2^\dagger \hat{a}_1), \tag{1}$$

where $\hat{a}_i$ is the bosonic annihilation operator for the ith well, χ represents the collisional nonlinearity, and J is the tunneling strength. We will always consider that the pumping is into well 1, which can be represented by the Hamiltonian

$$\mathcal{H}_{\rm pump} = i\hbar(\hat{\Gamma}\hat{a}_1^\dagger - \hat{\Gamma}^\dagger\hat{a}_1), \tag{2}$$

which is commonly used for the investigation of optical cavities. The basic assumption here is that the first well receives atoms from a condensate that is much larger than any of the modes in the wells we are investigating, so it will not become noticeably depleted over the time scales of interest. The damping term for well i acts on the system density matrix as the Lindblad superoperator

$$\mathcal{L}\rho = \gamma(2\hat{a}_i\rho\hat{a}_i^\dagger - \hat{a}_i^\dagger\hat{a}_i\rho - \rho\hat{a}_i^\dagger\hat{a}_i), \tag{3}$$

where γ is the coupling between the damped well and the atomic bath, which we assume to be unpopulated. Physically, such a damping process can be realized using an electron beam [3]. If the lost atoms fall under gravity, we are justified in using the Markov and Born approximations [25].

Following the usual procedures [26,27], we may map the problem onto a generalized Fokker-Planck equation (FPE) for the Wigner distribution of the system. Since this generalized FPE contains third-order derivatives, we truncate at second order. Although it is possible to map the third-order derivatives onto stochastic difference equations, these are highly unstable [28]. Having discarded these derivatives, we may map the resulting FPE onto Itô stochastic equations [29] for the Wigner variables. These equations for a two-well chain with pumping at well 1 and loss at well 2 are

$$\begin{aligned}\frac{d\alpha_1}{dt} &= \epsilon - 2i\chi|\alpha_1|^2\alpha_1 + iJ\alpha_2,\\ \frac{d\alpha_2}{dt} &= -\gamma\alpha_2 - 2i\chi|\alpha_2|^2\alpha_2 + iJ\alpha_1 + \sqrt{\gamma}\eta,\end{aligned} \tag{4}$$

with those with loss at the pumped well resulting from moving the terms proportional to γ. In the above equation, ϵ represents the rate at which atoms enter well 1 from the pumping mode, γ is the loss rate from the second well, and η is a complex Gaussian noise with the moments $\overline{\eta(t)} = 0$ and $\overline{\eta^*(t)\eta(t')} = \delta(t-t')$, where the overline represents a classical averaging process. The variables α_i correspond to the operators $\hat{a}_i$ in the sense that averages of products of the Wigner variables over many stochastic trajectories become equivalent to symmetrically ordered operator expectation values, for example, $\overline{|\alpha_i|^2} = \frac{1}{2}\langle\hat{a}_i^\dagger\hat{a}_i + \hat{a}_i\hat{a}_i^\dagger\rangle$. The initial states in all wells will be vacuum, sampled as in Ref. [30] for coherent states with vacuum excitation. We note here that we will use $\epsilon = 10$ and $\gamma = J = 1$ in all our numerical investigations, while varying the value of χ. We will consider three different χ values, 0, 0.001, and 0.01. The first represents noninteracting atoms and does not lead to any interesting quantum statistical features. The second is chosen as a smallish nonlinearity that will, however, lead to interesting quantum statistics. The third means that, for the pumping and loss rates we consider, we are approaching the single-mode limits of the Bose-Hubbard model, which depend on the ratio $\chi N/J$. We have averaged over at least 3×10^5 stochastic trajectories for all the graphical results presented here and the sampling error is typically less than the plotted linewidths.

III. QUANTITIES OF INTEREST

There are several quantities worthy of investigation here, including the populations in each well, $\overline{|\alpha_i|^2} - \frac{1}{2}$, the coherences between the wells, the currents into each well, the quadrature variances, a reduced single-particle pseudoentropy, and measures of separability and entanglement. We first define the real coherence function between wells 1 and 2,

$$\sigma_{12} = \sqrt{\langle\hat{a}_1^\dagger\hat{a}_2\rangle\langle\hat{a}_1\hat{a}_2^\dagger\rangle}. \tag{5}$$

Note that we define this as a real function so that it may be plotted, which is not as simple for the actual complex coherence, and take the square root so that it will be of the same magnitude as the currents. If our atomic cavities behave as a collection of superfluid states analogous to the electromagnetic field in a pumped optical cavity without internal nonlinearity, we expect that these would obtain their coherent-state values in the steady state, for example,

$$\sigma_{12} \to \overline{|\alpha_1||\alpha_2|}. \tag{6}$$

The inclusion of finite χ, with the attendant phase diffusion [15,19,31] and shearing of the Wigner function [32] to give non-Gaussian statistics, will act to decrease these values. The current from well 1 into well 2 is defined as

$$I_{12} = -i\langle\hat{a}_2^\dagger\hat{a}_1 - \hat{a}_1^\dagger\hat{a}_2\rangle. \tag{7}$$

Defining the atomic quadratures as

$$\hat{X}_j(\theta) = \hat{a}_j e^{-i\theta} + \hat{a}_j^\dagger e^{i\theta} \tag{8}$$

so that $\hat{Y}_j(\theta) = \hat{X}_j(\theta + \pi/2)$, squeezing exists whenever a quadrature variance is found to be less than 1, for any angle. As is well known, one of the effects of a $\chi^{(3)}$ nonlinearity is to cause any squeezing to be found at a nonzero quadrature angle [18]. Having defined our quadratures, we may now define the correlations we will investigate to detect entanglement between modes. The first of these, known as the Duan-Simon inequality [33,34], can be written so that, for any two separable states,

$$V(\hat{X}_j + \hat{X}_k) + V(\hat{Y}_j - \hat{Y}_k) \geqslant 4, \tag{9}$$

with any violation of this inequality demonstrating the inseparability of modes j and k.

A further set of inequalities, based on the Cauchy-Schwarz inequality, have been developed by Hillery and Zubairy [35]. They showed that, considering two separable modes denoted by i and j,

$$|\langle\hat{a}_i^\dagger\hat{a}_j\rangle|^2 \leqslant \langle\hat{a}_i^\dagger\hat{a}_i\hat{a}_j^\dagger\hat{a}_j\rangle, \tag{10}$$

with the equality holding for coherent states. The violation of this inequality is thus an indication of the inseparability of, and entanglement between, the two modes. As shown by Olsen [36–38], this is useful for systems where number conservation holds, in which case the Duan-Simon criterion may not detect inseparability. Although this is not the case here, it is still of interest to compare the predictions with

the quadrature inequalities defined above. Using the Hillery-Zubairy result, we now define the correlation function

$$\xi_{12} = \langle \hat{a}_1^\dagger \hat{a}_2 \rangle \langle \hat{a}_1 \hat{a}_2^\dagger \rangle - \langle \hat{a}_1^\dagger \hat{a}_1 \hat{a}_2^\dagger \hat{a}_2 \rangle \tag{11}$$

for which a positive value reveals entanglement between modes 1 and 2. In the Wigner representation, this is found as

$$\xi_{12} = \overline{\alpha_1^* \alpha_2} \times \overline{\alpha_2^* \alpha_1} - \overline{|\alpha_1|^2 |\alpha_2|^2} + \tfrac{1}{2}(\overline{|\alpha_1|^2 + |\alpha_2|^2}) - \tfrac{1}{4}. \tag{12}$$

The last quantity that we investigate is a pseudoentropy, derived from the single-particle reduced density matrix [19,39,40], defined for two wells as

$$\mathcal{R} = \frac{1}{\langle \hat{a}_1^\dagger \hat{a}_1 \rangle + \langle \hat{a}_2^\dagger \hat{a}_2 \rangle} \begin{bmatrix} \langle \hat{a}_1^\dagger \hat{a}_1 \rangle & \langle \hat{a}_1^\dagger \hat{a}_2 \rangle \\ \langle \hat{a}_2^\dagger \hat{a}_1 \rangle & \langle \hat{a}_2^\dagger \hat{a}_2 \rangle \end{bmatrix}. \tag{13}$$

The pseudoentropy is then defined in the standard von Neumann manner as

$$\mathcal{S} = -\mathrm{tr}(\mathcal{R} \ln \mathcal{R}). \tag{14}$$

Analytical values can be calculated in some limiting cases, such as a system of Fock or coherent states. These limiting cases are useful for the calculation of maximum values to which the system should relax if all coherences disappear. As a final note, we mention that all the quantities needed for the correlations above can in principle be measured, either by density (number) measurements or via atomic homodyning [41].

IV. PUMPING AND LOSS AT DIFFERENT WELLS

For a Bose-Hubbard dimer, there are two different configurations that we investigate. The first has pumping at well 1 with loss at well 2, while the second has both pumping and loss at well 1. As we show below, they exhibit qualitatively different behaviors.

A. Limits of an analytical approach

In order to demonstrate why we have proceeded using numerical phase-space methods, we will now investigate what is possible analytically. With the intracavity nonlinear coupler [18], which exhibits some similarities to the systems we investigate here, Olsen was able to find classical analytical solutions for the intensities and mode amplitudes. However, this depended to a large degree on the symmetry of the system, where both cavities had pumping and losses. The nonlinear component of an optical system is also degrees of magnitude smaller than that of an atomic system, so a linearized Gaussian fluctuation analysis can be reasonably accurate with the optical system. In general, we were not able to find exact analytical solutions for the mode amplitudes, except in the case of $\chi = 0$. In this particular case, everything remains completely classical, with no interesting quantum statistical features, as shown for Bose-Hubbard models without loss and pumping [36–38].

We now proceed by taking the classical version of Eq. (4),

$$\begin{aligned} \frac{d\alpha_1}{dt} &= \epsilon - 2i\chi |\alpha_1|^2 \alpha_1 + iJ\alpha_2, \\ \frac{d\alpha_2}{dt} &= -\gamma \alpha_2 - 2i\chi |\alpha_2|^2 \alpha_2 + iJ\alpha_1, \end{aligned} \tag{15}$$

which differs from Eq. (4) in that the α_i are now deterministic variables, not drawn from a statistical distribution, and there is no noise term associated with the loss from the second well. In the case of $\chi = 0$, we can solve for the steady states analytically,

$$\alpha_1 = \frac{\gamma \epsilon}{J^2}, \quad \alpha_2 = \frac{i\epsilon}{J}, \tag{16}$$

showing that the steady-state populations of the two wells are equal for our parameters, with the coherent excitation of the first well being real, while that of the second well is in the $\hat{Y}$ quadrature. For nonzero values of χ, we need to make approximations. One way of proceeding is to use the $\chi = 0$ steady-state solutions in the nonlinear terms, giving

$$\begin{aligned} \frac{d\alpha_1}{dt} &= \epsilon - 2i\chi N_1^{ss} \alpha_1 + iJ\alpha_2, \\ \frac{d\alpha_2}{dt} &= -\gamma \alpha_2 - 2i\chi N_2^{ss} \alpha_2 + iJ\alpha_1, \end{aligned} \tag{17}$$

where

$$N_1^{ss} = \frac{\gamma^2 \epsilon^2}{J^4}, \quad N_2^{ss} = \frac{\epsilon^2}{J^2}. \tag{18}$$

This allows us to find approximate steady-state solutions for the mode amplitudes

$$\begin{aligned} \alpha_1^{ss} &= \frac{\epsilon J^4 (\gamma J^2 + 2i\chi \epsilon^2)}{J^8 + 2i\chi J^2 \gamma^3 \epsilon^2 - 4\chi^2 \gamma^2 \epsilon^4}, \\ \alpha_2^{ss} &= \frac{i\epsilon J^7}{J^8 + 2i\chi J^2 \gamma^3 \epsilon^2 - 4\chi^2 \gamma^2 \epsilon^4}. \end{aligned} \tag{19}$$

As shown in Fig. 1, these solutions give reasonably accurate predictions for the steady-state atom numbers for the smaller nonlinearity $\chi = 10^{-3}$. They were also found to give the real and imaginary parts of the mode amplitudes to a similar accuracy. Unfortunately, for the higher nonlinearity $\chi = 10^{-2}$, with other parameters unchanged, they are completely inaccurate.

For the calculation of quantum statistical features, which is the main purpose of this article, they could possibly be useful for a linearized fluctuation analysis, at least for the lower nonlinearity. Unfortunately, such an analysis relies on the statistics of the system being Gaussian. In this case the statistics are non-Gaussian, as we see from the calculation of the third- and fourth-order cumulants κ_3 and κ_4, respectively [29,32], defined for an $\hat{X}$ quadrature as

$$\begin{aligned} \kappa_3(\hat{X}) &= \langle \hat{X}^3 \rangle + 2\langle \hat{X} \rangle^3 - 3\langle \hat{X} \rangle \langle \hat{X}^2 \rangle, \\ \kappa_4(\hat{X}) &= \langle \hat{X}^4 \rangle + 2\langle \hat{X} \rangle^4 - 3\langle \hat{X}^2 \rangle^2 - \langle \hat{X} \rangle \kappa_3(\hat{X}). \end{aligned} \tag{20}$$

We show the steady-state values for the first well, at zero quadrature angle, in Table I. As can be seen, they are nonzero, so the statistics are non-Gaussian. For these reasons, we will not proceed further with an analytical treatment.

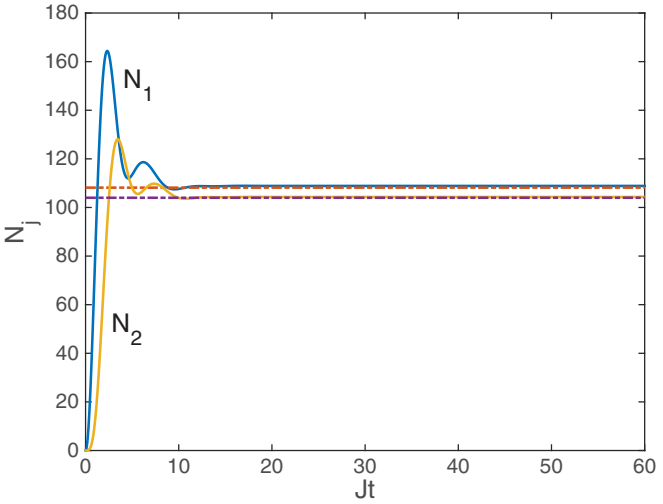

FIG. 1. Numerically calculated (solid lines) and approximately calculated analytical classical steady-state populations (dash-dotted lines) of the two wells with damping at well 2 and $\chi = 10^{-3}$. While these steady-state populations are reasonably accurate, those for higher χ values become totally inaccurate. Here Jt is a dimensionless time and all the quantities plotted in this and subsequent plots are dimensionless.

B. Stochastic quantum results

The configuration of this section is described by Eq. (4). For $\chi \neq 0$ we present the results of stochastic integration of the truncated Wigner equations. In Fig. 2 we show the stochastically calculated populations in the first well, for $\chi = 10^{-3}$ and 10^{-2}. The classical noninteracting steady-state solution is shown as a dashed line. We see that, while the smaller value of χ causes the steady-state value to increase, the larger value causes it to decrease. The values for the second well are shown in Fig. 3, where we see the same trend, so the total number of atoms decreases for the greater value of the nonlinearity. This is to be expected since the nonlinearity causes an imaginary component of the field analogous to that caused by detuning of an optical cavity, where the circulating power in an optical system decreases by a factor of $\gamma^2/(\gamma^2 + \Delta^2)$, where Δ is the detuning. The increase for the smaller χ value is counterintuitive and cannot be explained by the same reasoning.

The currents into the second well and the coherence functions σ_{12} are shown in Fig. 4. We see that increasing the collisional nonlinearity decreases both the current and the coherences. A decrease in current can be explained by the fact that, with the higher nonlinearity, we are approaching the macroscopic self-trapping regime [9,42–45], where tunneling is suppressed. The lower values of the coherences are explained

TABLE I. Steady-state values for the first well, at zero quadrature angle.

Cumulants	$\chi = 10^{-3}$	$\chi = 10^{-2}$
κ_3	-0.02	-0.3
κ_4	-1	-8

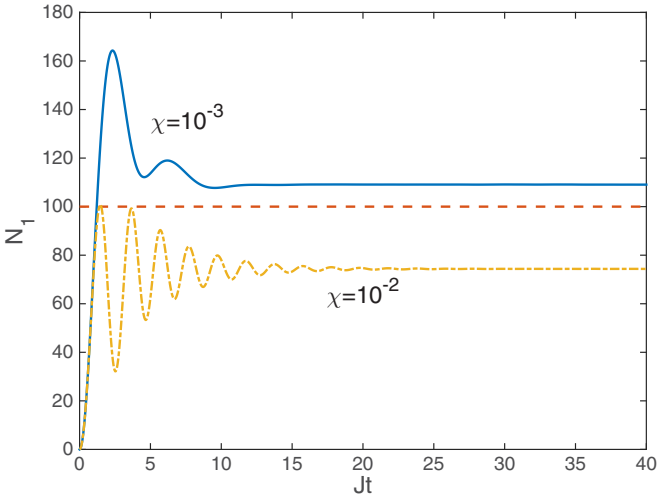

FIG. 2. Populations of the first well for different χ values and loss at well 2. The classical noninteracting value is shown by the dashed line.

almost entirely by the reduced populations, with phase diffusion playing a very limited role. Their values are almost indistinguishable from what is expected for two coherent states.

When we investigate the quantum statistics of the modes, we find steady-state quadrature squeezing and smallish violations of the Duan-Simon inequality of Eq. (9). We present these values and the quadrature angles of the greatest violation in Table II. We found that $\xi_{12} > 0$ only in the transient regimes, with no steady-state violations of the Hillery-Zubairy inequality. The steady-state pseudoentropy $\mathcal{S}$ was found to be 0.02 for $\chi = 10^{-3}$ and 0.07 for $\chi = 10^{-2}$. These low values are a result of the persistence of the off-diagonal coherences in the steady state, as can be seen in Eqs. (21) and (22). If the populations were equally distributed with no coherence between wells, we would find a value of $\log_2 \approx 0.6931$. For the actual mean populations, the values would be 0.6929 for $\chi = 10^{-3}$ and 0.6534 for $\chi = 10^{-2}$ if the coherences had

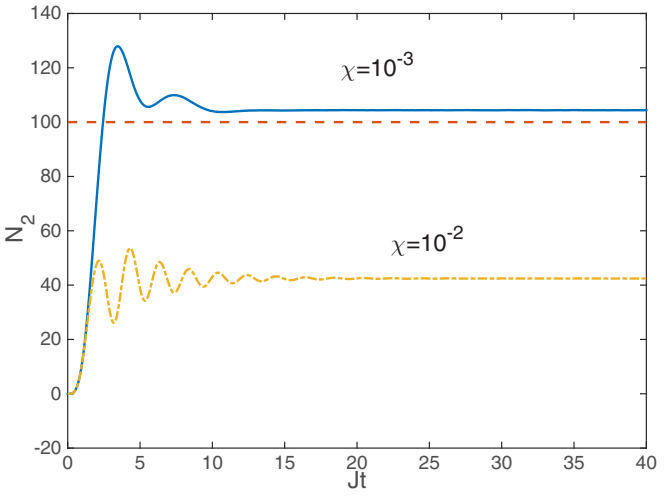

FIG. 3. Populations of the second well for different χ values and loss at well 2. The classical noninteracting value is shown by the dashed line.

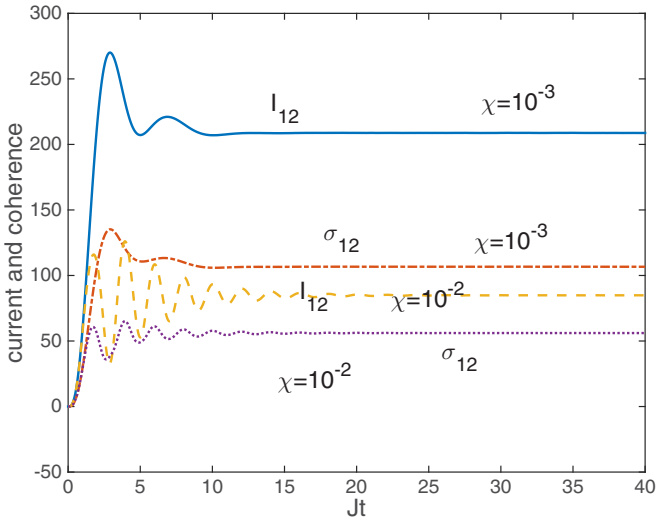

FIG. 4. Currents from well 1 into well 2 and the coherence function σ_{12} for two different values of χ.

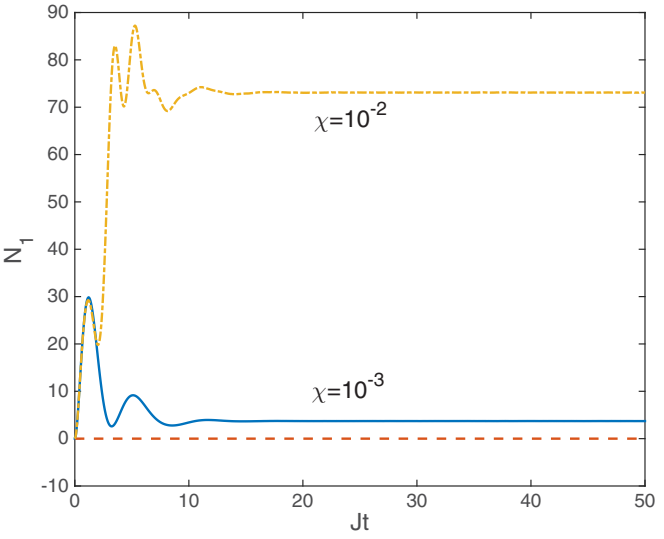

FIG. 5. Populations of the first well for two different different χ values and loss and pumping at well 1. The dashed line represents the classical noninteracting prediction.

disappeared. This is an indication that the populations in each well are close to coherent states. The actual steady-state reduced density matrices are found as

$$\mathcal{R}_{\chi=10^{-3}} = \begin{bmatrix} 0.51 & -0.10-0.49i \\ -0.10+0.49i & 0.49 \end{bmatrix} \tag{21}$$

and

$$\mathcal{R}_{\chi=10^{-2}} = \begin{bmatrix} 0.64 & -0.31-0.36i \\ -0.31+0.36i & 0.36 \end{bmatrix}. \tag{22}$$

V. PUMPING AND LOSS AT THE SAME WELL

This configuration has both pumping and dissipation at the first well. The classical steady-state solutions with $\chi = 0$ are found as

$$\alpha_1 = 0, \quad \alpha_2 = \frac{i\epsilon}{J}, \tag{23}$$

so the coherent excitation in the second well is again aligned with the $\hat{Y}$ quadrature. The first well, being a vacuum, has no preferred phase. It is interesting that the first well remains unoccupied in the steady state, with the tunneling between the two wells dropping to zero. As can be seen from Fig. 5, the addition of a finite χ changes this so that well 1 now has a nonzero steady-state occupation. The population of the second well is decreased over the noninteracting value, for both values of χ, as shown in Fig. 6. We also see that the total steady-state mean occupation of the system is unchanged by $\chi = 10^{-3}$, remaining at 100 atoms. With $\chi = 10^{-2}$, it increases to 129, which is again counterintuitive.

In Fig. 7 we show the real coherence functions and the tunneling for this configuration. We see that the steady-state tunneling goes to zero, which it must do to reach a state where the number in well 2 remains constant. Once again the steady-state coherence functions are indistinguishable from their coherent-state values. The fact that the higher value of χ results in larger magnitude coherences is entirely due to the increased total population and this is reflected in the steady-state pseudoentropy.

As with the previous configuration, we find that ξ_{12} only attains positive values in the transient regime. The other quantum statistical correlations are represented in Table III. We see that the quadrature squeezing results are similar to those of

TABLE II. Steady-state quadrature variances and values of the Duan-Simon correlation (9) as well as the quadrature angles of the minimal results.

Correlations	$\chi = 10^{-3}$	$\chi = 10^{-2}$
$V(\hat{X}_1)$	$0.65, 20^\circ$	$0.62, 122^\circ$
$V(\hat{X}_2)$	$0.78, 102^\circ$	$0.69, 2^\circ$
DS	$4.2, 33^\circ$	$3.9, 153^\circ$

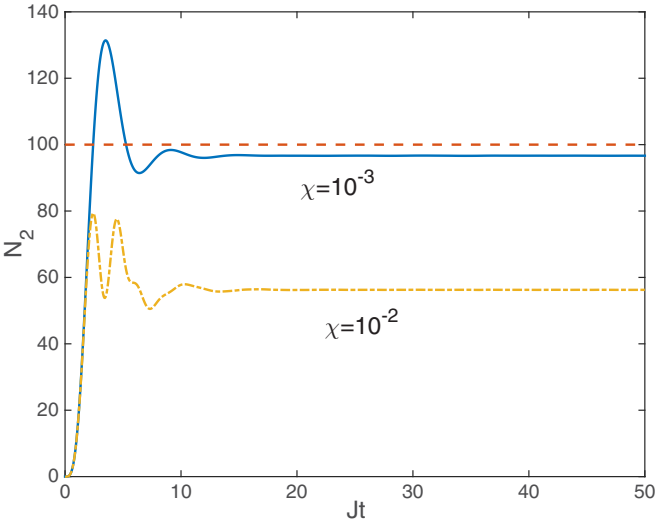

FIG. 6. Populations of the second well for the two different χ values and loss and pumping at well 1. The dashed line represents the classical noninteracting prediction.

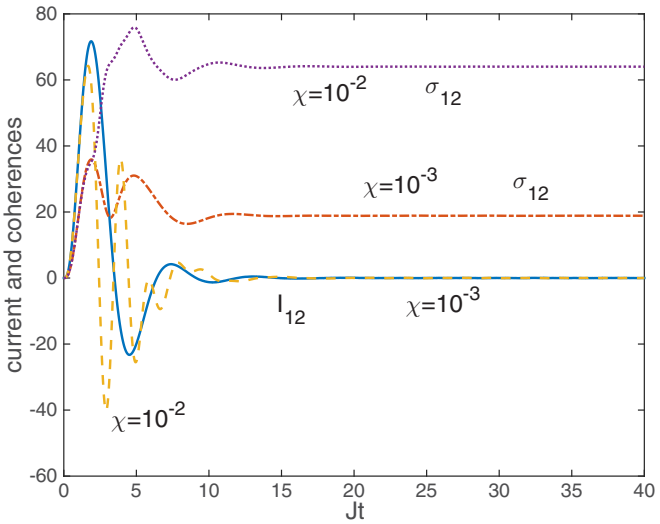

FIG. 7. Plot of I_{12} and σ_{12} for two different χ values, with both loss and pumping at well 1.

the first configuration, but that there is a significant violation of the Duan-Simon inequality for the higher nonlinearity. This can happen because the mode covariances are larger for these parameters. The steady-state pseudoentropy was found as 0.02 for $\chi = 10^{-3}$ and 0.03 for $\chi = 10^{-2}$. The actual steady-state reduced density matrices are found as

$$\mathcal{R}_{\chi=10^{-3}} = \begin{bmatrix} 0.04 & -0.19 \\ -0.19 & 0.96 \end{bmatrix} \tag{24}$$

and

$$\mathcal{R}_{\chi=10^{-2}} = \begin{bmatrix} 0.57 & -0.49 \\ -0.49 & 0.43 \end{bmatrix}. \tag{25}$$

With zero coherences and unchanged populations, the values of the pseudoentropy would be 0.17 and 0.68, respectively. We see that, for both configurations, the intracavity systems are far from their closed-system equilibrium values. The increased violation of the Duan-Simon inequality for the higher nonlinearity, and over the first system that we considered, suggests that this system may be the better one for any experimental measurement of bipartite mode entanglement.

TABLE III. Quantum statistical correlations.

Correlations	$\chi = 10^{-3}$	$\chi = 10^{-2}$
$V(\hat{X}_1)$	0.88, 13°	0.67, 160°
$V(\hat{X}_2)$	0.74, 109°	0.72, 151°
DS	3.9, 115°	2.8, 155°

VI. CONCLUSION

We have analyzed the quantum dynamics of a pumped and damped Bose-Hubbard dimer in two different configurations. Depending on which well is damped, the population dynamics were found to be very different. The inclusion of a finite collisional term in the equations of motion changes the average solutions from their noninteracting values. In particular, in the second configuration we analyzed, with pumping and damping at the same well, collisions cause a finite steady-state population in the first well by contrast to the zero occupation predicted without collisional interaction. Our model would be very difficult to achieve in coupled cavity optics, where loss is inevitable in both pumped and unpumped resonators.

Going beyond the populations, we have found squeezing in the steady-state atomic quadratures, with the amount of squeezing increasing as the collisional nonlinearity is increased. The only configuration for which we found a reasonable entanglement signal between the two wells was for the higher nonlinearity and pumping and damping at different wells. Our calculations of a reduced single-particle pseudoentropy show that the systems remain far from the equilibrium state of two isolated wells, with the interwell coherences not dropping markedly below those expected for coherent states. Given recent experimental advances, an experimental realization of these systems should be possible. As a final remark, we note that the truncated Wigner method that we have used easily allows for extension to a greater number of wells.

ACKNOWLEDGMENTS

This research was supported by the Australian Research Council under the Future Fellowships Program (Grant No. FT100100515) and the Brazilian Conselho Nacional de Desenvolvimento Científico e Tecnológico.

[1] K. Henderson, C. Ryu, C. MacCormick, and M. G. Boshier, New J. Phys. **11**, 043030 (2009).
[2] G. Gauthier, I. Lenton, N. McKay Parry, M. Baker, M. J. Davis, H. Rubinsztein-Dunlop, and T. W. Neely, arXiv:1605.04928v1.
[3] R. Labouvie, B. Santra, S. Heun, S. Wimberger, and H. Ott, Phys. Rev. Lett. **115**, 050601 (2015).
[4] C. Weitenberg, M. Endres, J. F. Sherson, M. Cheneau, P. Schauß, T. Fukuhara, I. Bloch, and S. Kuhr, Nature (London) **471**, 319 (2011).
[5] G. Kordas, D. Witthaut, and S. Wimberger, Ann. Phys. (Leipzig) **527**, 619 (2015).
[6] G. Kordas, D. Witthaut, P. Buonsante, A. Vezzani, R. Burioni, A. I. Karanikas, and S. Wimberger, Eur. Phys. J. Spec. Top. **224**, 2127 (2015).
[7] H. Gersch and G. Knollman, Phys. Rev. **129**, 959 (1963).
[8] D. Jaksch, C. Bruder, J. I. Cirac, C. W. Gardiner, and P. Zoller, Phys. Rev. Lett. **81**, 3108 (1998).
[9] G. J. Milburn, J. F. Corney, E. M. Wright, and D. F. Walls, Phys. Rev. A **55**, 4318 (1997).
[10] P. D. Drummond and D. F. Walls, J. Phys. A **13**, 725 (1980).
[11] I. Pižorn, Phys. Rev. A **88**, 043635 (2013).
[12] A. Le Boité, G. Orso, and C. Ciuti, Phys. Rev. Lett. **110**, 233601 (2013).
[13] B. Cui, S. C. Hou, W. Wang, and X. X. Yi, J. Phys. B **47**, 215303 (2014).
[14] R. Graham, in *Quantum Statistics in Optics and Solid-State Physics*, edited by G. Höhler, Springer Tracts in Modern Physics Vol. 66 (Springer, Berlin, 1973), pp. 1–97.

[15] M. J. Steel, M. K. Olsen, L. I. Plimak, P. D. Drummond, S. M. Tan, M. J. Collett, D. F. Walls, and R. Graham, Phys. Rev. A **58**, 4824 (1998).
[16] P. D. Drummond and C. W. Gardiner, J. Phys. A **13**, 2353 (1980).
[17] J. F. Corney and M. K. Olsen, Phys. Rev. A **91**, 023824 (2015).
[18] M. K. Olsen, Phys. Rev. A **73**, 053806 (2006).
[19] C. V. Chianca and M. K. Olsen, Phys. Rev. A **84**, 043636 (2011).
[20] M. K. Olsen, K. Dechoum, and L. I. Plimak, Opt. Commun. **190**, 261 (2001).
[21] M. J. Davis, S. J. Thwaite, M. K. Olsen, and K. V. Kheruntsyan, Phys. Rev. A **77**, 023617 (2008).
[22] A. Vardi and J. R. Anglin, Phys. Rev. Lett. **86**, 568 (2001).
[23] J. R. Anglin and A. Vardi, Phys. Rev. A **64**, 013605 (2001).
[24] D. Witthaut, F. Trimborn, H. Hennig, G. Kordas, T. Geisel, and S. Wimberger, Phys. Rev. A **83**, 063608 (2011).
[25] G. M. Moy, J. J. Hope, and C. M. Savage, Phys. Rev. A **59**, 667 (1999).
[26] C. W. Gardiner and P. Zoller, *Quantum Noise* (Springer-Verlag, Heidelberg, 2000).
[27] D. F. Walls and G. J. Milburn, *Quantum Optics* (Springer-Verlag, Berlin, 1995).
[28] L. I. Plimak, M. K. Olsen, M. Fleischhauer, and M. J. Collett, Europhys. Lett. **56**, 372 (2001).
[29] C. W. Gardiner, *Stochastic Methods: A Handbook for the Natural and Social Sciences* (Springer-Verlag, Berlin, 2002).
[30] M. K. Olsen and A. S. Bradley, Opt. Commun. **282**, 3924 (2009).
[31] M. Lewenstein and L. You, Phys. Rev. Lett. **77**, 3489 (1996).
[32] M. K. Olsen and J. F. Corney, Phys. Rev. A **87**, 033839 (2013).
[33] L.-M. Duan, G. Giedke, J. I. Cirac, and P. Zoller, Phys. Rev. Lett. **84**, 2722 (2000).
[34] R. Simon, Phys. Rev. Lett. **84**, 2726 (2000).
[35] M. Hillery and M. S. Zubairy, Phys. Rev. Lett. **96**, 050503 (2006).
[36] C. V. Chianca and M. K. Olsen, Phys. Rev. A **92**, 043626 (2015).
[37] M. K. Olsen, Phys. Rev. A **92**, 033627 (2015).
[38] M. K. Olsen, Opt. Commun. **371**, 1 (2016).
[39] M. P. Strzys and J. R. Anglin, Phys. Rev. A **81**, 043616 (2010).
[40] C. V. Chianca and M. K. Olsen, Phys. Rev. A **83**, 043607 (2011).
[41] A. J. Ferris, M. K. Olsen, E. G. Cavalcanti, and M. J. Davis, Phys. Rev. A **78**, 060104 (2008).
[42] K. Nemoto, C. A. Holmes, G. J. Milburn, and W. J. Munro, Phys. Rev. A **63**, 013604 (2000).
[43] R. Franzosi and V. Penna, Phys. Rev. A **65**, 013601 (2001).
[44] A. P. Hines, R. H. McKenzie, and G. J. Milburn, Phys. Rev. A **67**, 013609 (2003).
[45] M. Albiez, R. Gati, J. Folling, S. Hunsmann, M. Cristiani, and M. K. Oberthaler, Phys. Rev. Lett. **95**, 010402 (2005).